Electronic Supplementary Information to

Cell Shapes and Patterns are Quantitative Indicators of Tissue Mechanics

submitted to Soft Matter

Sangwoo Kim and Sascha Hilgenfeldt,

Mechanical Science and Engineering, University of Illinois, Urbana-Champaign

June 23, 2015

In this Supporting Information, we provide additional details on the tissue mechanics simulations, as well as on tests of the robustness and generality of the results outlined in the main text.

1 Global orientation of cells

When we combine the novel findings on tissue mechanics with our earlier results on the correlations of tissue statistics and cell shapes [1, 2], it is important to acknowledge that those results were only considering local cell environments, and thus no long-range correlations of cells shapes or orientations. If large-scale directional forces act on a tissue, they will generally induce cells to collectively align in a certain direction, which would lead to very different statistics. Even if there is no large-scale directional force, in a given mechanical situation a tissue sample (in experiment or simulation) might be able to minimize its energy by spontaneously breaking symmetry and orienting cells in a (random) preferential global direction. Both cases would lead to a peak in the distribution of cell orientation angles ϕ_i (indicating the long axis of the equivalent ellipse). We found that our samples of cucumber epidermal tissues show no conclusive signature of such large-scale organization (Fig. S1a).

Hence, the anisotropy in cucumber tissues is not an artifact of global effects such as anisotropic stress along the fruit growth direction. We do not include any energy term related to such global stress in the mechanical model, and the image analysis results from the simulations confirm that the orientation of individual cells is random here as well, i.e., no spontaneous symmetry breaking occurs (Fig. S1b).

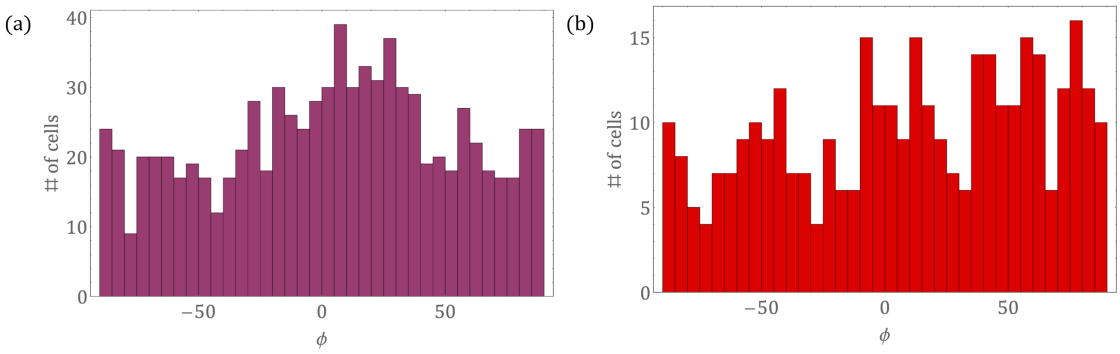

Figure S1: Frequency graphs (with equal number of bins) of orientation angle ϕ of cells in (a) a *Cucumis* tissue sample in experiment, (b) a sample in a Surface Evolver simulation, with the same polydispersity $c_A = 0.38$ as the experiment. In this simulation, $c_P = 0.045$, $\gamma = 0.22$, so that the sample is at the transition point.

2 Different form of the energy functional

We tested how sensitive an equilibrium state is to different functional forms of the dependence of mechanical energy on the cellular perimeters, while maintaining the generic leading-order behavior represented by the quadratic energy functional Eq. 2 of the main text. One strong variation is to let the energy vary exponentially with the perimeter. Using the average perimeter $\bar{P} = 2(\pi\bar{A})^{1/2}$, we obtain

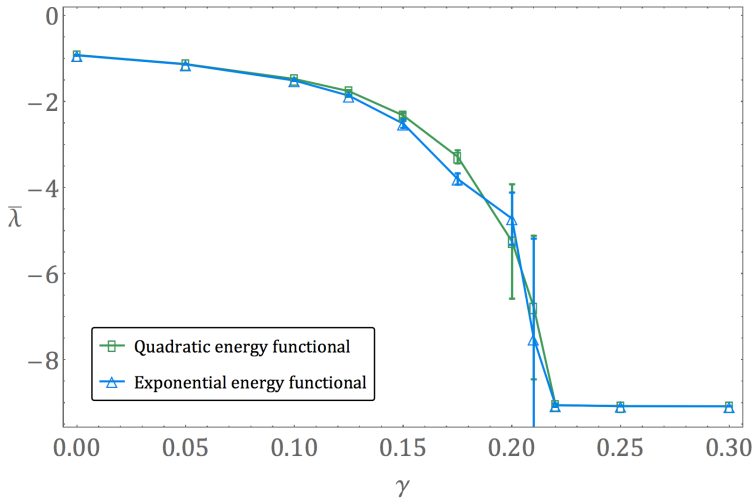

Figure S2: Dependence of average tension $\bar{\lambda}$ on γ for the quadratic and exponential energy functionals, for monodisperse samples with $c_P = 0.045$. While the variability of $\bar{\lambda}$ near γ_c is somewhat different, both curves track each other very closely, and the transition value γ_c itself is indistinguishable.

the following energy functional that coincides with Eq. 2 to leading order:

$$E_{exp} = \sum_{i=1}^{N} \bar{P} \exp\left[\frac{1}{2}\frac{(P_i - (1+\frac{\gamma}{2})P_{i,0})^2}{P_{i,0}\bar{P}}\right] \tag{1}$$

Conducting simulations, we find that the exponential energy functional generates an almost identical transition curve $\bar{\lambda}(\gamma)$, see Fig. S2. This confirms that the SE simulation result is insensitive to the exact form of the energy functional, not just at the transition γ_c itself (where this is necessitated by construction), but for all relevant values of $\gamma - \gamma_c$.

3 Bending energy

Quenched disorder that arises naturally from biological systems plays an important role in reproducing the correct shape distributions in our model. However, a higher degree of quenched disorder (in the equilibrium perimeters $P_{i,0}$ of the cells) also generates strongly curved edges in the equilibrium configuration, with a degree of curvature that is not observed in cucumber epidermal tissues. This deformation mode is accessible to the cells in our model because there is no resistance to bending in the energy functional. A bending energy term for edge ij of type $E_{bend,ij} = (1/2)K_b C_{ij}^2 L_{ij}$ with the edge curvature C_{ij} is introduced to investigate this issue. Note that this is a term that goes beyond the leading-order energy functional for structureless (one-dimensional) boundaries between cells – bending energy implies a finite

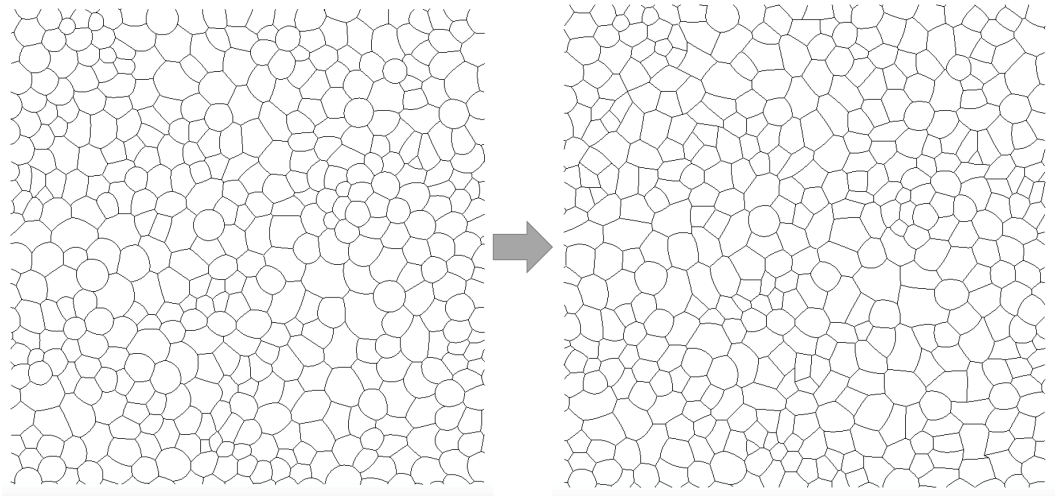

Figure S3: Equilibrium configurations from SE simulations; (a) using the energy functional of Eq. 2 in the main text, without a bending energy term. (b) using the energy functional with the added bending energy (1). The curvature in the edges is reduced compared to (a), while the geometric and statistical features given in the figures remain in very close agreement.

width h of the cell-cell interface. For our normalization of the energy functionals (they are divided by the area stretch modulus K_A), the simple result is $K_b = h^2/12$ from the mechanics of plate bending [3]. The cell wall thickness h is measurable from experimental images as $h \approx 1.0\mu$m, so that the bending energy functional does not introduce any additional free parameters. SE simulations including $E_{bend,ij}$ show that the large edge curvatures are relieved, but the shape distribution and statistics are virtually unchanged (cf. Fig. S3). Simulations for γ values both far from and near the transition show changes in $\bar{e}$ by only about 2%, and the width of $P(e)$ changes by less than 4%. Likewise, the value of c_n changes less than 4% when bending energy is included, well within the range of experimental uncertainty. We conclude that bending energy has a negligible effect on the conclusions of the present work, and adopt Eq. 2 of the main text to optimize computational effort.

4 Dependence of the transition value of γ on simulational degrees of freedom

Are the conclusions about the transition from tense to relaxed tissues at γ_c dependent on the protocol and method of the simulations? One certainly needs to check whether the transition is robust against changes of shape refinement: Surface Evolver determines the lowest-energy geometric configuration given the functional of Eq. 2 of the main text, but this local minimum is in general dependent on the refinement (degrees of freedom). Two simple implementations are the linear model (with straight edges between all vertices) and the quadratic model (with piecewise parabolic edges). In addition, every edge element can be further refined, increasing the number of degrees of freedom to almost arbitrary resolution. Figure S4 shows a schematic of cells for these models (beyond the linear model, the extra vertices along edges represent the extra degrees of freedom).

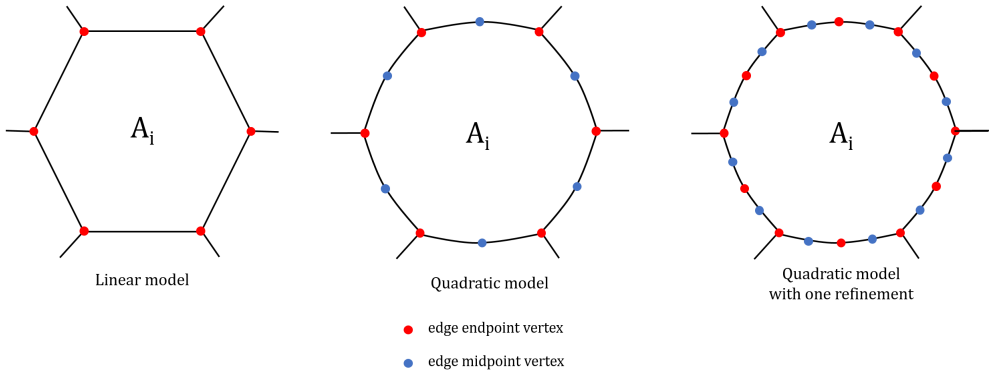

Figure S4: Schematic of nodes (degrees of freedom in energy minimization) for the different SE models discussed in the text.

In general, we would expect that more refinement yields a more realistic model (as the simulational system is closer to exploring the continuum degrees of freedom of the real physical system), and that the state of minimal energy changes. We found that this is true, but only significant with respect to the first refinement from linear to quadratic model. Conducting simulations with different refinement models, but otherwise identical distributions, we find that the transition persists, but the transition value of γ is strongly different for the linear model even in the case of monodisperse cells with no perimeter disorder (where the edges tend to be straighter in models with more degrees of freedom). Figure S5 demonstrates that this transition value γ_0 (for $c_A = 0$, $c_P = 0$), determined as the γ where all edge tensions drop below the numerical-accuracy threshold, moves from $\gamma_0 \approx 0.155$ in the linear model to $\gamma_0 \approx 0.125$ in the quadratic model. Therefore, the linear model does not provide enough degrees of freedom for a realistic transition. Equally importantly, if the number of degrees of freedom is increased further by implementing edge refinement, the additional effect is entirely negligible. The transition value γ_0 changes by about 10^{-4} upon introducing two steps of refinement for all edges and minimizing the energy. Hence, we conclude that further refinement has almost no effect on the transition value, and we adopt the unrefined quadratic model for all simulations.

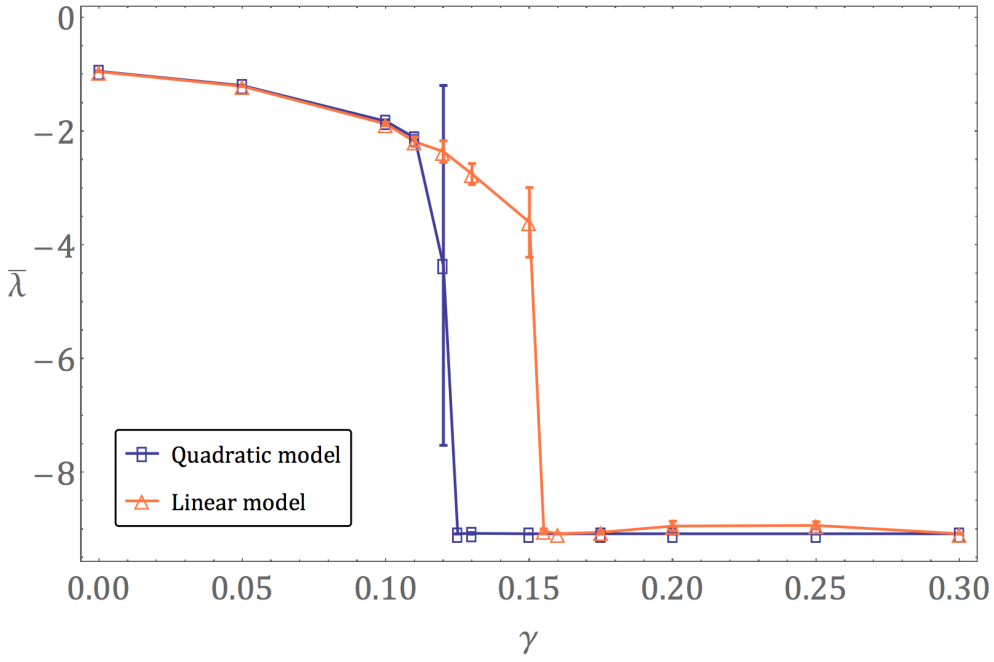

Figure S5: Comparison of $\bar{\lambda}(\gamma)$ for the linear and quadratic models, for otherwise identical monodisperse samples without quenched disorder ($c_A = 0, c_P = 0$). Note the significant changes in the location of the transition value γ_0, while further refinement results in no distinguishable changes to the quadratic-model transition value.

5 Variability of tension and protocol dependence

It can be seen in the graphs of $\bar{\lambda}(\gamma)$ (Fig. 3a of the main text) that the average tension values are very well defined both for small γ and for $\gamma > \gamma_c$ (beyond the transition). It is in the approach to transition, where tension vanishes precipitously, that large fluctuations appear in the $\bar{\lambda}$ value of the individual samples, leading to the large standard deviation error bars. Note that the average $\bar{\lambda}$ still decreases very systematically, approaching zero in a power-law fashion. The most striking property of the variability, though, is that it is not reflected within each sample: Figure S6 shows the probability distributions of the tension measures λ of individual edges ($\lambda_{ij} = \log \epsilon_{ij}^{eff}$) for five polydisperse samples without disorder ($c_P = 0$) near transition ($\gamma = 0.13$). All distributions are reasonably narrow, but their mean values vary over an extremely wide range (note that two of these samples actually reached zero tension to numerical accuracy ($\bar{\lambda} < \bar{\lambda}_{min}$), but we have not bounded the values to illustrate the range of tensions). Quantitatively, the average coefficient of variation c_λ of $P(\lambda)$ within single samples is 0.09. This value increases to 0.32 when the same test is performed with the observed degree of disorder ($c_P = 0.045$), but is still far less than the variation from sample to sample.

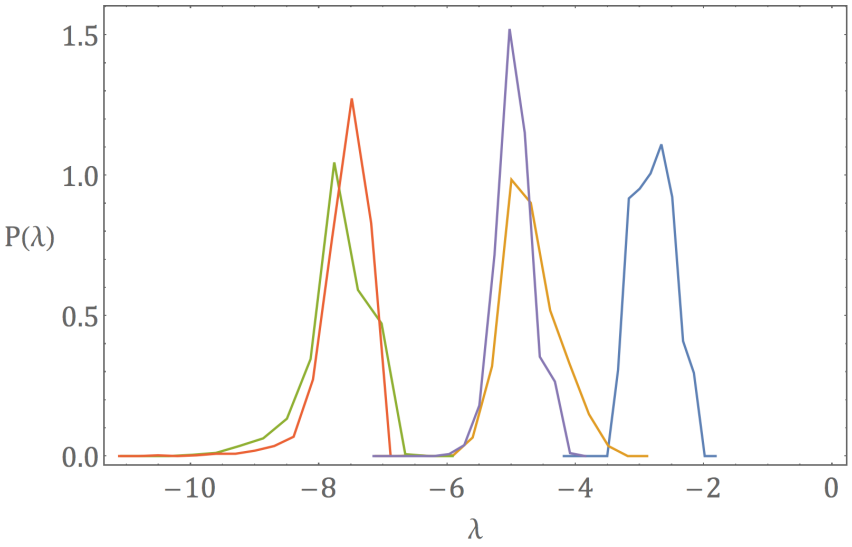

Figure S6: Probability distribution $P(\lambda)$ of logarithmic strains for five samples with different initial conditions, but identical parameters: all samples are polydisperse ($c_A = 0.38$), without quenched disorder ($c_P = 0$), and near the transition ($\gamma = 0.13$). The variation between the mean λ values of different samples is much greater than the variation within each sample.

We therefore conclude that the sample size of $N = 400$ used in the simulations is small enough to give rise to very significant variations in mechanical ground states given the individual initial conditions. This is confirmed by changes in the T1 protocols, which may significantly change the $\bar{\lambda}$ values of individual samples, but do not eliminate this strong sample-to-sample variation. A realistic system of finite size

would be subject to the same variability of local energy minima. As a consequence, in order to be certain that a given sample reaches a relaxed, zero-tension state, the parameter γ has to be large enough so that the tension drops to zero (or below the numerical threshold of accuracy) for all samples. This explains why the geometry and statistics of our tissue samples are compatible with γ values at γ_c, but not smaller γ (where a considerable relief of tension could already be expected, but not for all realizations).

References

[1] Miklius, M. P & Hilgenfeldt, S. (2012) Analytical results for size-topology correlations in 2d disk and cellular packings. *Phys. Rev. Lett.* **108**, 015502.

[2] Kim, S, Cai, M, & Hilgenfeldt, S. (2014) Lewis' law revisited: the role of anisotropy in size–topology correlations. *New Journal of Physics* **16**, 015024.

[3] Landau, L, Pitaevskii, L, Kosevich, A, & Lifshitz, E. (2012) *Theory of Elasticity.* (Elsevier Science) No. v. 7.